Supporting Information

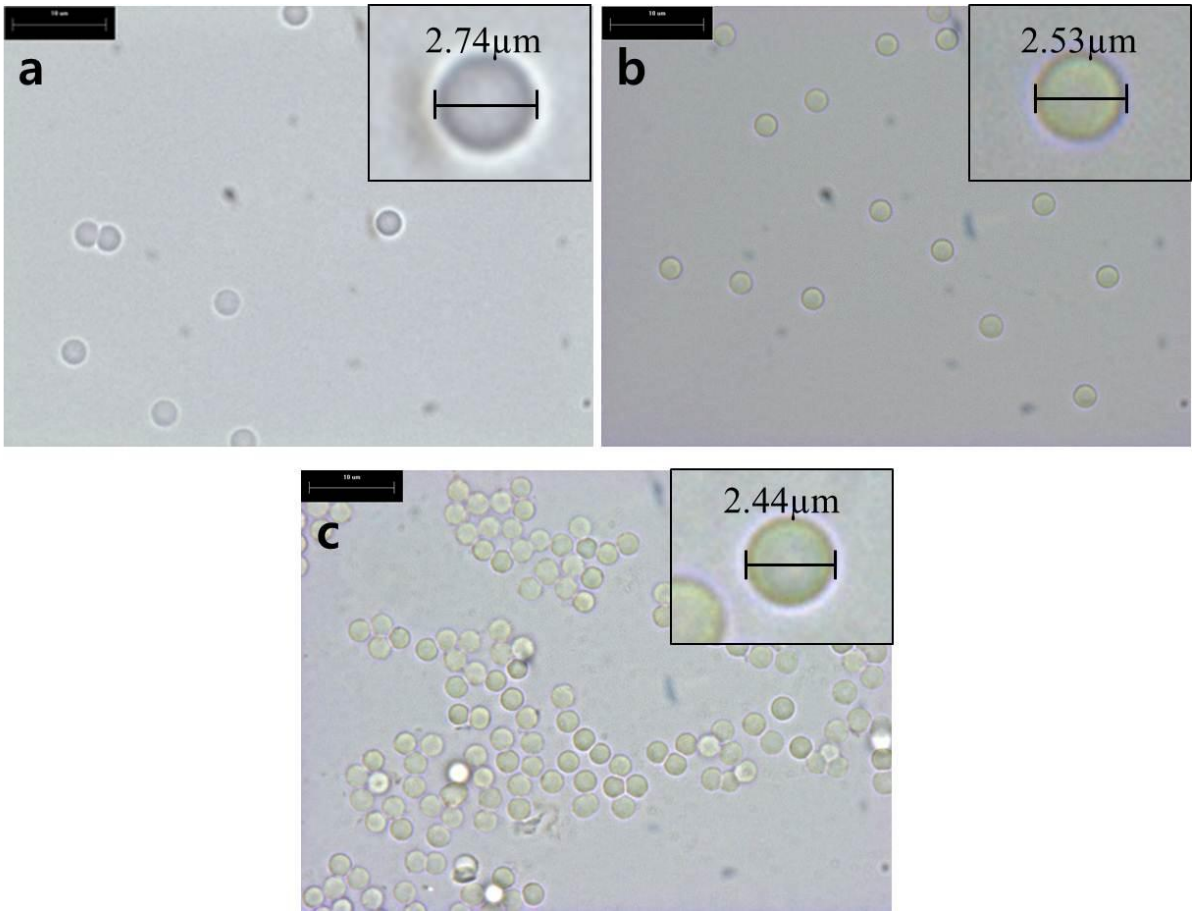

Figure S1

Figure S1. OM images of the synthetic process for Fe metal precursor/poly(MAA/EGDMA) composite microspheres: (a) swollen poly(MAA/EGDMA) microspheres, (b) after adding $FeSO_4 \cdot 7H_2O_2$ (c) after stirring for 12h with reduction agent.

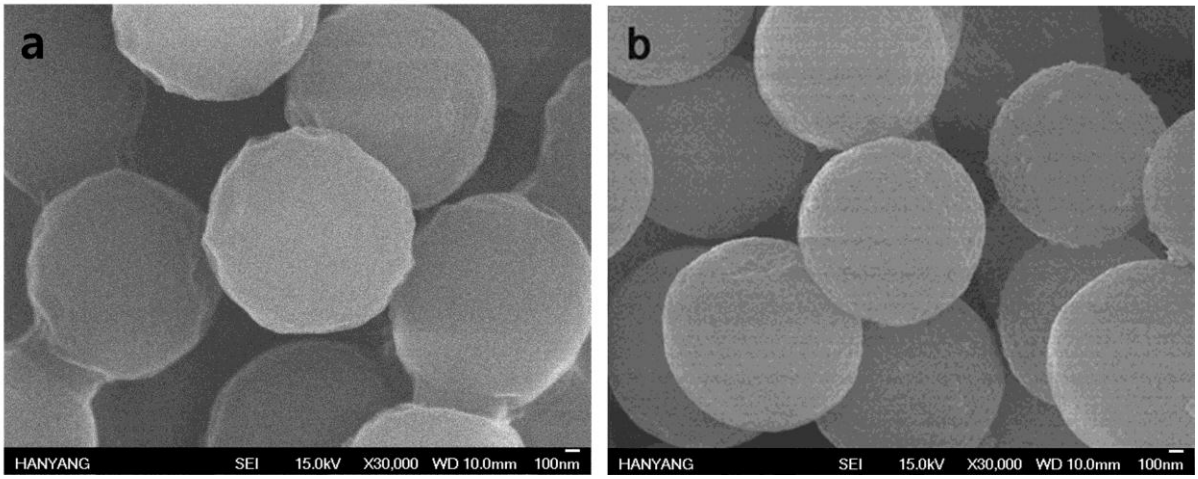

Figure S2

Figure S2. SEM images of (a) poly(MAA/EGDMA) microspheres and (b) Fe metal precursor/poly(MAA/EGDMA) composite microspheres.

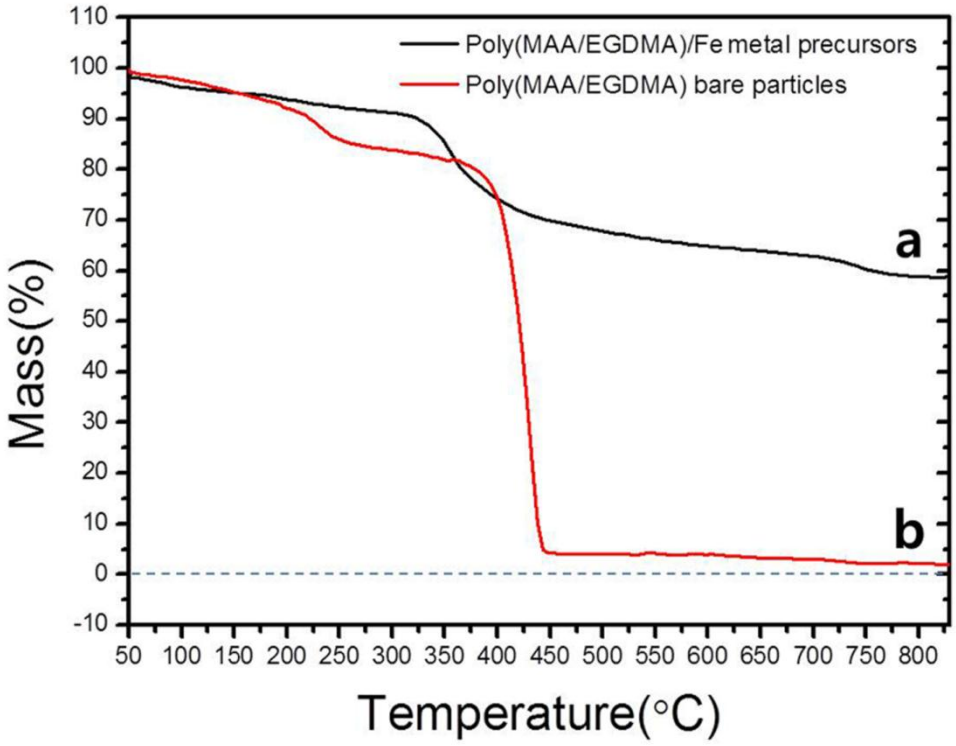

Figure S3

Figure S3. TGA curves of (a) Fe metal precursors/poly(MAA/EGDMA) composite microspheres and (b) poly(MAA/EGDMA) microspheres.

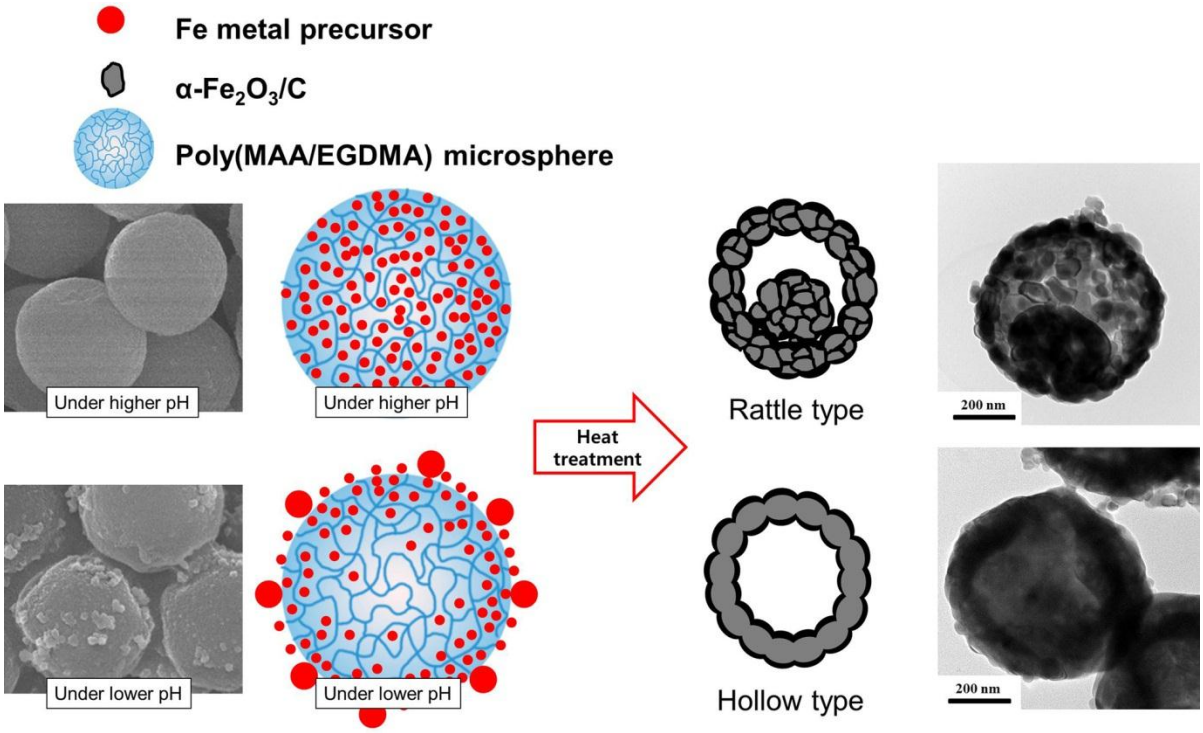

Figure S4

Figure S4. (c) Schematic illustration of formation process of hollow and rattle-type Fe_2O_3/C submicron spheres by heat treatment. SEM images of Fe metal precursors/poly(MAA/EGDMA) microspheres prepared under different pH ((a) 7.05 and (b) 6.07) value of exterior solution and TEM images of two types of Fe_2O_3/C ((d) rattle and (e) hollow) submicron spheres after heat treatment.

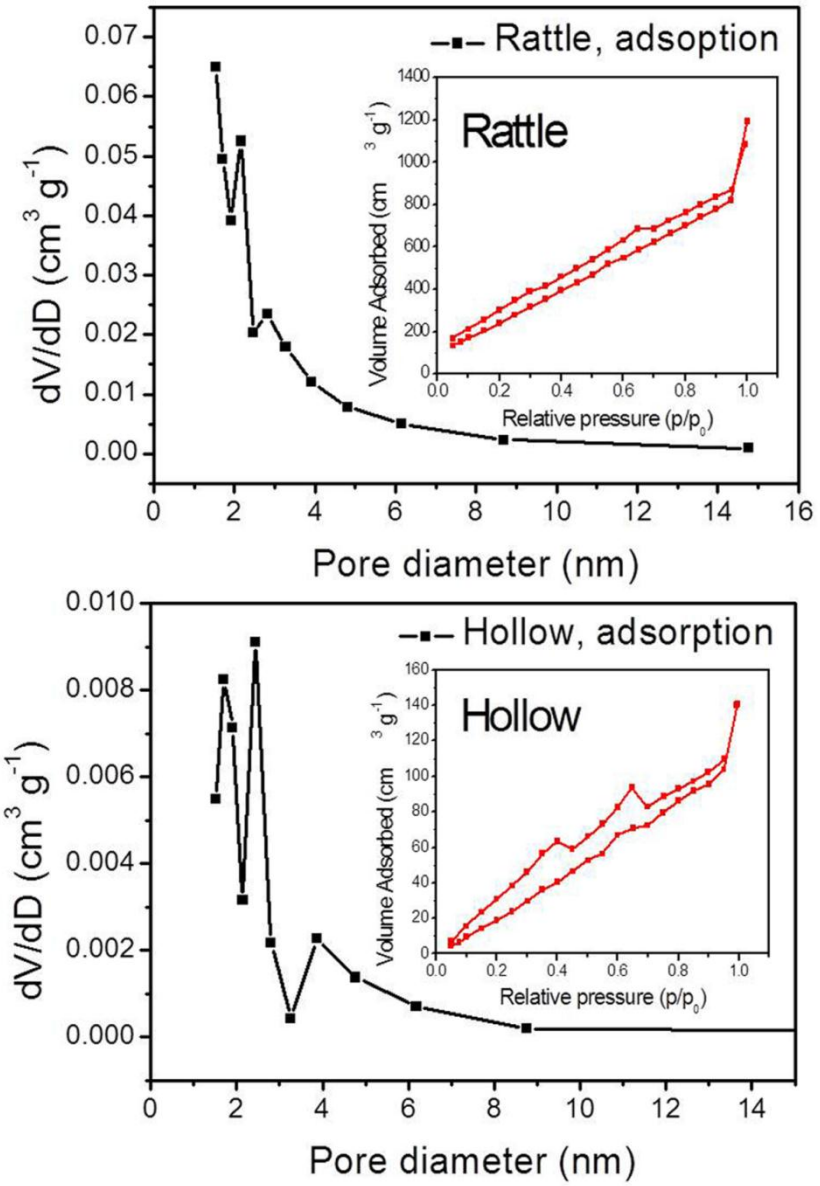

Figure S5

Figure S5. Pore size distribution and the nitrogen sorption isotherms (insets) of the hollow and rattle-type α-Fe_2O_3/C submicron spheres

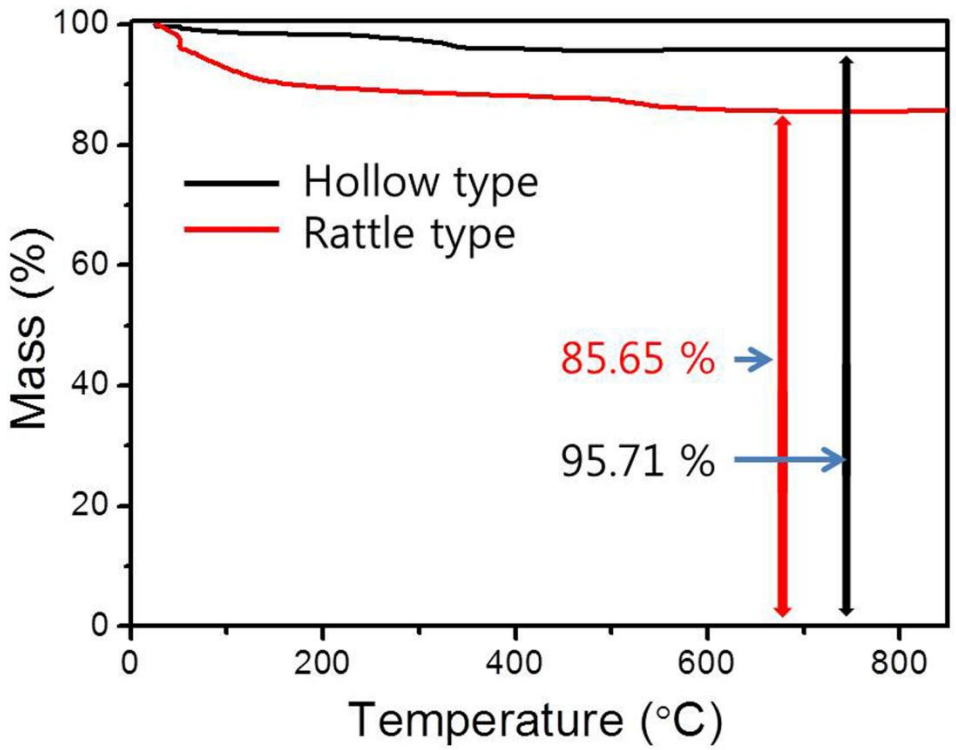

Figure S6

Figure S6. TGA curves of the hollow and rattle-type α-Fe_2O_3/C submicron spheres with air flow at a heating rate of 5°C min^{-1}.